JOURNAL OF SOLID STATE CHEMISTRY **126,** 292–299 (1996)
ARTICLE NO. 0340

Hydrothermal Syntheses and Structures of Three-Dimensional Oxo-fluorovanadium Phosphates: $[H_2N(C_2H_4)_2NH_2]_{0.5}[(VO)_4V(HPO_4)_2(PO_4)_2F_2(H_2O)_4] \cdot 2H_2O$ and $K_2[(VO)_3(PO_4)_2F_2(H_2O)] \cdot H_2O$

Grant Bonavia,* R. C. Haushalter,† and Jon Zubieta*

*Department of Chemistry, Syracuse University, Syracuse, New York 13244; †NEC Research Institute, 4 Independence Way, Princeton, New Jersey 08540

Received February 26, 1996; in revised form June 21, 1996; accepted June 26, 1996

The hydrothermal reactions of FPO_3H_2 with vanadium oxides result in the incorporation of fluoride into V–P–O frameworks as a consequence of metal-mediated hydrolysis of the fluorophosphoric acid to produce F^- and PO_4^{3-}. By exploiting this convenient source of F^-, two 3-dimensional oxo-fluorovanadium phosphate phases were isolated, $[H_2N(C_2H_4)_2NH_2]_{0.5}[(VO)_4V(HOP_4)_2(PO_4)_2F_2(H_2O)_4] \cdot 2H_2O$ ($1 \cdot 2H_2O$) and $K_2[(VO)_3(PO_4)_2F_2(H_2O)] \cdot H_2O$ ($2 \cdot H_2O$). Both anionic frameworks contain $(V^{IV}O)$–F^--phosphate layers, with confacial bioctahedral $\{(V^{IV}O)_2FO_6\}$ units as the fundamental motif. In the case of 1, the layers are linked through $\{V^{III}O_6\}$ octahedra, while for 2 the interlayer connectivity is provided by edge-sharing $\{(V^{IV}O)_2F_2O_6\}$ units. Crystal data are $1 \cdot 2H_2O$, $CH_{10}FN_{0.5}O_{13}P_2V_{2.5}$, monoclinic $C2/m$, $a = 18.425(4)$ Å, $c = 8.954(2)$ Å, $\beta = 93.69(2)^0$, $V = 1221.1(4)$ Å^3, $Z = 4$, $D_{calc} = 2.423$ g cm^{-3}; $2 \cdot H_2O$, $H_4F_2K_2O_{13}P_2V_3$, triclinic $P\bar{1}$, $a = 7.298(1)$ Å, $b = 8.929(2)$ Å, $c = 10.090(2)$ Å, $\alpha = 104.50(2)^0$, $\beta = 100.39(2)^0$, $\delta = 92.13(2)^0$, $V = 623.8(3)$ Å^3, $Z = 2$, $D_{calc} = 2.891$ g cm^{-3}. © 1996 Academic Press, Inc.

The contemporary interest in the vanadium phosphate system derives from the catalytic applications of the vanadyl pyrophosphate, $[(VO)_2P_2O_7]$, in the selective oxidation of butane to maleic anhydride (1–5). In recent years, a number of ''naked'' oxovanadium phosphate phases (6–14), as well as V–P–O materials incorporating a variety of heterometal cations and exhibiting one- (15–19), two- (20–28), or three-dimensional structures (29–52), have been characterized. The extensiveness of the chemistry of the M^{n+}–V–P–O system reflects the versatility of the vanadium centers in adopting different oxidation states and coordination geometries and the ability of the phosphate group to exhibit different protonated forms and varying numbers of pendant {P=O} subunits.

It has also been demonstrated that the structural diversity of the V–P–O system may be further enhanced by introducing organoammonium cations as templates for the preparation of microporous materials (53–61). In this respect, it has been noted for the well-documented microporous frameworks derived from the $AlPO_4$ and $GaPO_4$ families that partial substitution of oxo-groups by fluoride anions results in even more varied coordination types (62–64). This observation led to the discovery of the first microporous fluorovandophosphate, $(H_3NCH_2CH_2NH_3)[(VO_2)_2F(PO_4)]$, by Riou and Férey (65).

In the course of our investigations of the V–P–O system, we sought to incorporate fluoride into the anionic framework as a potential means of enhancing the thermal stability of these materials. While introduction of fluoride by employing HF in our syntheses proved relatively unsatisfactory, we have found that the metal-mediated hydrolysis of FPO_3H_2 provides a means of facile incorporation of F^- into V–P–O frameworks. In this paper, we report the syntheses and structures of two unusual fluorovanadophosphates, the mixed valance V(III)/V(IV) material $[H_2N(C_2H_4)_2NH_2][(VO)_4V(HPO_4)_2(PO_4)_2F_2(H_2O)_4] \cdot 2H_2O$ ($\mathbf{1} \cdot 2H_2O$) and the V(IV) species $K_2[(VO)_3(PO_4)_2F_2(H_2O)] \cdot H_2O$($\mathbf{2} \cdot H_2O$).

EXPERIMENTAL

Experimental procedures. Reactants were purchased from commercial sources and used without further purification. All syntheses were carried out in Teflon-lined Parr acid digestion bombs under autogenous pressure. The reactants were stirred briefly before heating. The reaction vessels were filled to approximately 40% volume capacity.

Synthesis of $[H_2N(C_2H_4)_2NH_2]_{0.5}[(VO)_4V(HPO_4)_2(PO_4)_2F_2(H_2O)_4] \cdot 2H_2O$ ($\mathbf{1} \cdot 2H_2O$). A mixture of V_2O_5 (0.030 g), piperazine (0.071 g), FPO_3H_2 (0.12 mL, 70%; $D = 1.830$ g/mL), and water (3 mL) in the mole ratio 1.00 : 5.01 : 9.33 : 1001 was heated at 200°C for 44 h. Light blue plates of **1** were collected in 67% yield based on vanadium. IR (KBr pellet, cm^{-1}): 3484 (m), 3186 (m), 1609 (m), 1435 (m), 1135 (s), 1051 (s), 960 (m), 579 (m),

0022-4596/96 $18.00

TABLE 1
Crystal Data and Details of the X-Ray Data Collections of $[H_2N(C_2H_4)NH_2]_{0.5}$ $[V(VO)_4(HPO_4)_2(PO_4)_2F_2(H_2O)_4] \cdot 2H_2O$ (1 · $2H_2O$) and $K_2[(VO)_3(PO_4)_2F_2(H_2O)] \cdot H_2O$ (2 · H_2O)

	1 · $2H_2O$	2 · H_2O
Empirical formula	$C_2H_{10}N_{0.5}O_{13}P_2V_{2.5}$	$H_4O_{13}F_2P_2K_2V_3$
Formula ugt.	459.4	543.0
Space group	$C2/m$	$P\bar{1}$
a (Å)	18.425(4)	7.298(1)
b (Å)	7.417(1)	8.929(2)
c (Å)	8.954(2)	10.090(2)
α (°)	—	104.50(3)
β (°)	93.69(2)	100.39(3)
γ (°)	—	92.13(3)
V (Å^3)	1221.1(4)	623.8(1)
Z	4	2
D calc (g cm^{-3})	2.499	2.891
T (K)	296	295
Wavelength	0.71073 (MoKα)	0.71073 (Mo$K\alpha$)
Scan mode	2θ	2θ
Scan rate	4.0 to 12.0°/min	4.0 to 12.0°/min
Absorption coefficient (cm^{-1})	22.39	25.01
Absorption correction	ψ-scans	ψ-scans
T_{max}/T_{min}	1.03/0.86	0.97/0.82
$F(000)$	880	526
Crystal dimensions (mm)	0.34 × 0.22 × 0.20	0.12 × 0.13 × 0.11
2θ range (°)	4.0 to 45.0	4.0 to 60.0
hkl range	$0 \geq h \geq 25$	$-10 \geq h \geq 10$
	$0 \geq k \geq 10$	$0 \geq k \geq 12$
	$-12 \geq l \geq 12$	$-14 \geq l \geq 13$
Reflections collected	1908	3853
Reflections used ($I_0 \geq 3\sigma(I_0)$)	892	2786
Number of parameters	104	199
Final Fourier residuals	−1.16 to 1.15	−0.78 to 1.38
Goodness of fit	1.54	1.88
R_1	0.063	0.044
R_2	0.067	0.051

532 (m). Anal. calcd. for $C_2H_{20}NO_{26}F_2P_4V_5$: V, 28.1. Found: 28.0.

Synthesis of $K_2[(VO)_3(PO_4)_2F_2(H_2O)] \cdot H_2O$ (**2** · H_2O). A mixture of KVO_3 (0.023 g), dimethylamine (0.13 mL, 40% in H_2O), FPO_3H_2 (0.07 mL, 70% in H_2O) and H_2O) and H_2O (3 mL) was heated at 200·C for 48 h. Light blue plates of **2** · H_2O were collected in 73% yield based on vanadium. IR(BKr pellet, cm^{-1}): 3474 (m), 1648 (w), 1099 (s), 1023 (m), 948 (s), 804 (m). Anal. calcd. for $H_4O_{13}F_2P_2K_2V_3$: V, 28.2. Found: V, 28.3.

X-ray crystallographic studies. Structural measurements for complexes **1** · $2H_2O$ and **2** · H_2O were performed on a Rigaku AFC5S diffractometer with graphite monochromated Mo$K\alpha$ radiation [λ(Mo-Kα) = 0.71073 Å]. The data were collected at a temperature of 20 ± 1°C using the ω-2θ scan technique.

Crystallographic data for these compounds are listed in Table 1. The intensities of three standard reflections measured after every 150 reflections remained constant throughout the data collections. An empirical absorption correction using the program DIFABS was applied to all data [66], and the data were corrected for Lorentz and polarization effects. The structures were solved by direct methods [67]. Vanadium, phosphorus, and oxygen atoms were refined anisotropically. Neutral atom scattering factors were taken from Cromer and Weber [68] and the anomalous dispersion correction was taken from those of Creagh and McAuley [69]. All calculations were performed using the SHELXTL [70] crystallographic software package.

For phosphate **1** · $2H_2O$, the piperazinium cation sites were present at half occupancies, with the carbon backbones disordered about two positions in equal occupancies. Successful refinement of the positional and thermal parameters of the piperazinium group and the absence of anomalous bond distances and of excursions of electron density confirmed the adequacy of the model. Oxygen atoms O8 and O9 are also disordered about the 2/m site occupied by V2. Attempts to refine the structure as an ordered model in the acentric space groups $C2$ or Cm produced unrealistic thermal parameters and large correlation coefficients. The model reported was considered appropriate.

RESULTS AND DISCUSSION

The incorporation of fluoride into the V–P–O frameworks of **1** · $2H_2O$ and **2** · H_2O was accomplished by

TABLE 2
Atomic Positional Parameters (×10^4) and Isotropic Temperature Factors (Å^2 × 10^3) for $[H_2N(C_2H_4)_2NH_2]_{0.5}[(VO)_4V(HPO_4)_2(PO_4)_2F_2(H_2O)_4] \cdot 2H_2O$ (1 · $2H_2O$)

	x	y	z	U(eq)
V(1)	2286(1)	2052(2)	7454(2)	10(1)
V(2)	5000	0	10000	21(2)
P(1)	3263(2)	0	5073(4)	8(1)
P(2)	3269(2)	0	10106(4)	8(1)
F	1451(4)	0	7325(8)	14(2)
O(1)	3959(5)	0	6201(10)	15(3)
O(2)	2582(5)	0	5989(9)	10(3)
O(3)	1689(3)	3280(9)	5843(6)	14(2)
O(4)	2597(4)	0	8933(9)	9(3)
O(5)	1745(3)	3289(8)	8971(6)	13(2)
O(6)	3963(5)	0	9241(9)	11(3)
O(7)	3043(3)	3101(10)	7475(7)	20(2)
O(8)	5050(9)	−2462(25)	9192(18)	48(5)
O(9)	4723(8)	995(24)	11893(18)	47(5)
O(10)	4017(5)	5000	9681(11)	26(3)
N(1)	0	1965(35)	5000	20(5)
C(1)	728(10)	822(29)	4739(21)	22(4)
C(1A)	4604(11)	4157(31)	6142(26)	34(6)

Note: Equivalent isotropic U defined as one third of the trace of the orthogonalized U_{ij} tensor.

exploiting the metal-mediated hydrolysis of FPO_3H_2 to produce F^- and PO_4^{3-}. While no mechanistic conclusions can be drawn on the basis of product analysis alone, fluorophosphoric acid does not undergo appreciable hydrolysis under hydrothermal conditions in the absence of a vanadium source. This observation confirms a role for the vanadium in mediating the hydrolysis process and suggest that fluoride coordination to the vanadium sites is one consequence of this reaction. While the use of HF and H_3PO_4 in place of FPO_3H_2 in the reactions does allow isolation of **1** and **2**, the yields are considerably diminished, in the 5–20% range. This observation suggests that the metal-mediated hydrolysis of FPO_3H_2 produces F^- in close proximity to the V(IV) sites, thereby forming a repository of fluoride-bonded vanadium sites.

The appearance of bands in the 3100–3500 cm^{-1} range for **1** · $2H_2O$ confirmed the presence of water in the solid. The bands in the 1000–1200 cm^{-1} range are attributed to ν(P–O) of the phosphate, while the sharp feature at 960 cm^{-1} is associated with ν(V=O). The infrared spectrum of **2** · H_2O exhibits similar characteristics features: 3474 cm^{-1}, ν(O—H); 1099 and 1023 cm^{-1}, ν(P–O); and 948 cm^{-1}, ν(V=O).

X-ray structural analysis of **1** · $2H_2O$ revealed a complex three-dimensional structure with cavities occupied by the organic cations and water molecules of crystallization. The overall structure of the anionic framework may be described as V–P–F–O layers, containing octahedral V(IV) binuclear units as the fundamental building blocks, linked through V(III) octahedra, as shown in Fig. 1. The V(IV) binuclear motifs are present as face-sharing octahedra shown in Fig. 2a, rather than the more common edge- or corner-sharing units. The coordination geometry about each V(IV) center is defined by a terminal oxo-group, a bridging fluoride ligand, two phosphate oxygen donors in a bridging ligation mode, and two terminal phosphate oxygen donors. The bridging fluoride adopts as orientation *trans* to the terminal oxo-group, a geometry reflected in the long V–F distance of 2.163(5) Å, resulting from the strong *trans* influence of the oxo-groups. Each $\{V_2F_2O_8\}$ confacial bioctahedral unit is linked to four adjacent binuclear units in the layer through bridging phosphate groups, as shown in Fig. 2b.

There are two distinct phosphate units, as depicted in Fig. 3a. The P1 site contributes one oxygen donor to the

TABLE 3

Atomic Positional Parameters (×10^4) and Isotropic Temperature Factors (Å^2 × 10^3) for $K_2[(VO)_3(PO_4)_2F_2(H_2O)]$ · H_2O (2 · H_2O)

	x	*y*	*z*	*U*(eq)
V(1)	351(1)	2277(1)	4587(1)	5(1)
V(2)	3232(1)	3665(1)	9166(1)	8(1)
V(3)	5558(1)	−2436(1)	5422(1)	5(1)
K(1)	1404(2)	4671(2)	2288(1)	17(1)
K(2)	7954(2)	1221(2)	7783(1)	21(1)
P(1)	2988(2)	451(1)	6539(1)	5(1)
P(2)	2801(2)	5431(1)	6516(1)	5(1)
F(1)	3826(4)	5629(4)	10667(3)	11(1)
F(2)	8026(4)	−1925(3)	7009(3)	9(1)
O(1)	1181(5)	−393(4)	6652(4)	9(1)
O(2)	4591(5)	−586(4)	6466(4)	9(1)
O(3)	2596(5)	1031(4)	5176(4)	6(1)
O(4)	3629(5)	1796(4)	7811(4)	10(1)
O(5)	4701(5)	6334(4)	6634(4)	8(1)
O(6)	2810(5)	4903(4)	7824(4)	10(1)
O(7)	2520(5)	4032(4)	5191(4)	7(1)
O(8)	1162(5)	6427(4)	6381(4)	10(1)
O(9)	−366(5)	2561(4)	6028(4)	11(1)
O(10)	1082(5)	3358(5)	9331(4)	16(1)
O(11)	4043(5)	−2976(5)	3988(4)	13(1)
O(12)	4284(6)	2379(5)	10581(4)	16(1)
O(13)	2402(9)	9267(7)	9610(6)	38(2)

Note. Equivalent isotropic *U* defined as one third of the trace of the orthogonalized U_{ij} tensor.

TABLE 4

Selected Bond Lengths (Å) and Angles (°) for $[H_2N(C_2H_4)_2NH_2]_{0.5}$ $[(VO)_4V(HPO_4)_2(PO_4)_2F_2(H_2O)_4]$ · $2H_2O$ (1 · $2H_2O$)

V(1)–F	2.163(5)	V(1)–O(2)	2.104(6)
V(1)–O(3)	1.979(6)	V(1)–O(4)	2.074(6)
V(1)–O(5)	1.964(6)	V(1)–O(7)	1.596(7)
V(1)–V(1A)	3.044(3)	V(2)–O(6)	1.987(8)
V(2)–O(8)	1.969(18)	V(2)–O(9)	1.947(17)
P(1)–O(1)	1.582(9)	P(1)–O(2)	1.543(9)
P(1)–O(3)	1.522(6)	P(1)–O(3A)	1.522(6)
P(2)–O(4)	1.572(8)	P(2)–O(6)	1.536(9)
P(2)–O(5)	1.516(6)	P(2)–O(5A)	1.516(6)
N(1)–C(1)	1.616(23)	C(1)–C(1A)	1.568(30)
F–V(1)–O(2)	70.7(3)	F–V(1)–O(3)	85.7(2)
O(2)–V(1)–O(3)	91.9(3)	F–V(1)–O(4)	71.6(3)
O(2)–V(1)–O(4)	78.2(3)	O(3)–V(1)–O(4)	157.1(3)
F–V(1)–O(5)	88.5(3)	O(2)–V(1)–O(5)	158.9(3)
O(3)–V(1)–O(5)	90.3(2)	O(4)–V(1)–O(5)	91.9(3)
F–V(1)–O(7)	164.2(3)	O(2)–V(1)–O(7)	95.7(3)
O(3)–V(1)–O(7)	103.2(3)	O(4)–V(1)–O(7)	98.4(3)
O(5)–V(1)–O(7)	104.2(3)	O(6)–V(2)–O(8)	86.6(5)
O(6)–V(2)–O(9)	89.8(5)	O(8)–V(2)–O(9)	133.9(7)
O(6)–V(2)–O(6A)	180.0(1)	O(8)–V(2)–O(6A)	93.4(5)
O(9)–V(2)–O(6A)	90.2(5)	O(6)–V(2)–O(8)	86.6(5)
O(8)–V(2)–O(8)	136.1(9)	O(9)–V(2)–O(8)	89.4(7)
O(6)–V(2)–O(8)	93.4(5)	P(1)–P(1)–O(2)	108.3(5)
O(1)–P(1)–O(3)	105.8(3)	O(2)–P(1)–O(3)	111.3(3)
O(1)–P(1)–O(3A)	105.8(3)	O(2)–P(1)–O(3A)	111.3(3)
O(3)–P(1)–O(3A)	113.9(5)	O(4)–P(2)–O(6)	108.0(5)
O(4)–P(2)–O(5)	108.9(3)	O(6)–P(2)–O(5)	108.6(3)
O(4)–P(2)–O(5A)	108.9(3)	O(6)–P(2)–O(5A)	108.6(3)
O(5)–P(2)–O(5A)	113.7(5)	V(1)–F–V(1A)	89.5(3)
V(1)–O(2)–P(1)	125.7(3)	V(1)–O(2)–V(1A)	92.7(3)
P(1)–O(2)–V(1A)	125.7(3)	V(1)–O(3)–P(1)	136.9(4)
V(1)–O(4)–P(2)	126.9(3)	V(1)–O(4)–V(1A)	94.4(3)
P(2)–O(4)–V(1)	126.9(3)	V(1)–O(5)–P(2)	142.7(4)

TABLE 5
Selected Bond Lengths (Å) and Angles (°) for $K_2[(VO)_3(PO_4)_2F_2(H_2)] \cdot H_2O$(2 · H_2O)

V(1)–O(3)	2.096(4)	V(1)–O(7)	2.079(3)
V(1)–O(9)	1.598(4)	V(1)–F(2)	2.135(3)
V(1)–O(1)	1.986(3)	V(1)–O(8)	1.946(4)
V(2)–F(1)	1.983(3)	V(2)–O(4)	1.943(4)
V(2)–O(6)	1.943(4)	V(2)–O(10)	1.627(4)
V(2)–O(12)	2.106(5)	V(2)–F(1A)	2.180(3)
V(3)–F(2)	2.133(3)	V(3)–O(2)	1.955(4)
V(3)–O(11)	1.607(4)	V(3)–O(3)	2.074(4)
V(3)–O(5)	1.998(4)	V(3)–O(7)	2.097(4)
K(1)–O(7)	3.095(4)	K(1)–F(1)	2.857(4)
K(1)–F(2)	2.744(4)	K(1)–O(5)	3.103(4)
K(1)–O(6)	3.098(4)	K(1)–O(8)	2.775(4)
K(1)–O(9)	2.841(4)	K(1)–O(10)	2.882(4)
K(1)–O(10A)	3.109(5)	K(1)–O(11)	2.787(4)
K(1)–O(12)	3.381(5)	K(2)–F(2)	2.726(3)
K(2)–O(2)	2.801(4)	K(2)–O(4)	3.221(4)
K(2)–F(1)	3.294(3)	K(2)–O(1)	3.054(4)
K(2)–O(3)	3.102(3)	K(2)–O(9)	2.795(5)
K(2)–O(10)	2.862(4)	K(2)–O(11)	2.900(5)
K(2)–O(13)	2.826(7)	P(1)–O(1)	1.531(4)
P(1)–O(2)	1.519(4)	P(1)–O(3)	1.571(4)
P(1)–O(4)	1.510(3)	P(2)–O(5)	1.549(4)
P(2)–O(6)	1.507(4)	P(2)–O(7)	1.561(3)
P(2)–O(8)	1.523(4)		
O(3)–V(1)–O(7)	79.8(1)	O(3)–V(1)–O(9)	95.5(2)
O(7)–V(1)–O(9)	98.6(2)	O(3)–V(1)–F(2)	72.5(1)
O(7)–V(1)–F(2)	72.2(1)	O(9)–V(1)–F(2)	165.7(2)
O(3)–V(1)–O(1)	93.5(1)	O(7)–V(1)–O(1)	156.2(2)
O(9)–V(1)–O(1)	104.9(2)	F(2)–V(1)–O(1)	84.0(1)
O(3)–V(1)–O(8)	160.0(2)	O(7)–V(1)–O(8)	89.0(2)
O(9)–V(1)–O(8)	102.6(2)	F(2)–V(1)–O(8)	88.4(2)
O(1)–V(1)–O(8)	90.1(2)	F(1)–V(2)–O(4)	159.2(1)
F(1)–V(2)–O(6)	88.2(1)	O(4)–V(2)–O(6)	94.6(2)
F(1)–V(2)–O(10)	96.4(2)	O(4)–V(2)–O(10)	103.5(2)
O(6)–V(2)–O(10)	99.0(2)	F(1)–V(2)–O(12)	90.9(1)
O(4)–V(2)–O(12)	82.1(2)	O(6)–V(2)–O(12)	167.9(2)
O(10)–V(2)–O(12)	93.1(2)	F(1)–V(2)–F(1A)	73.5(1)
O(6)–V(2)–F(1B)	84.2(1)	O(10)–V(2)–F(1)	169.3(2)
O(12)–V(2)–F(1)	83.9(2)	F(2)–V(3)–O(2)	87.9(1)
F(2)–V(3)–O(11)	166.3(2)	O(2)–V(3)–O(11)	103.5(2)
F(2)–V(3)–O(3)	72.9(1)	O(2)–V(3)–O(3)	89.7(2)
O(11)–V(3)–O(3)	99.2(2)	F(2)–V(3)–O(5)	83.2(1)
O(2)–V(3)–O(5)	90.2(2)	O(11)–V(3)–O(5)	104.0(2)
O(3A)–V(3)–O(5)	156.2(1)	F(2)–V(3)–O(7)	71.8(1)
O(2)–V(3)–O(7)	159.2(1)	O(11)–V(3)–O(7)	96.0(2)
O(3)–V(3)–O(7)	79.9(1)	O(5)–V(3)–O(7)	92.1(2)
O(1)–P(1)–O(3)	108.1(2)	O(2)–P(1)–O(3)	108.8(2)
O(1)–P(1)–O(4)	110.3(2)	O(2)–P(1)–O(4)	106.2(2)
O(3)–P(1)–O(4)	110.8(2)	O(5)–P(2)–O(6)	109.3(2)
O(5)–P(2)–O(7)	107.7(2)	O(6)–P(2)–O(7)	111.9(2)
O(5)–P(2)–O(8)	112.6(2)	O(6)–P(2)–O(8)	106.5(2)
O(7)–P(2)–O(8)	108.9(2)	V(2)–F(1)–V(2A)	106.5(1)
V(3)–F(2)–V(1)	88.8(1)	P(1)–O(1)–V(1C)	131.7(2)
V(3)–O(2)–P(1)	146.8(2)	V(1)–O(3)–P(1)	125.9(2)
V(1)–O(3)–V(3)	91.4(2)	P(1)–O(3)–V(3)	125.6(2)
V(2)–O(4)–P(1)	153.0(2)	P(2)–O(5)–V(3)	131.2(2)
V(2)–O(6)–P(2)	160.8(3)	V(1)–O(7)–P(2)	125.6(2)
V(1)–O(7)–V(3B)	91.2(1)	P(2)–O(7)–V(3B)	128.1(2)
P(2)–O(8)–V(1B)	150.9(3)		

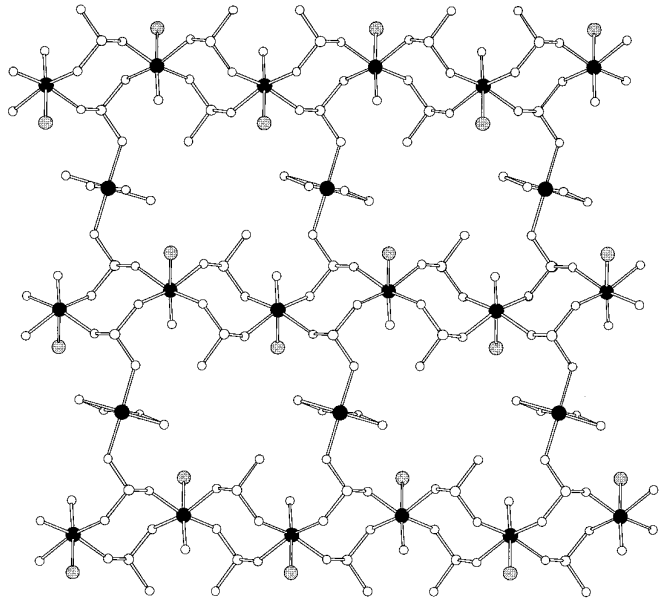

FIG. 1. A ball and stick representation of the structure of the anionic framework of **1**, illustrating the $V^{IV}O$–F^-–phosphate layers linked by $\{V^{III}O_6\}$ octahedra. Vanadium sites are solid black spheres; fluoride sites are grey spheres.

bridge between two V(IV) sites of a binuclear unit. Two oxygen donors serve to bridge to each of two adjacent binuclear units in a monodentate fashion, while the fourth oxygen is protonated and pendant. The P1–O1 distance of 1.582(9) Å is considerably longer than the average 1.524(8) Å of all other P–O distances in **1** · $2H_2O$, confirming its identity on the protonation site and that of the P1 unit as a hydrophosphate, $(HPO_4)^{2-}$. The P2 site is present on a $(PO_4)^{3-}$ unit. In a similar fashion to the P1 site, the P2 tetrahedron contributes one oxygen donor to the bridge between V(IV) centers of a binuclear unit and utilizes two oxygen donor to bridge to each of two adjacent vanadium motifs in the layer. However, in contrast to P1, the fourth oxygen is used to bond to the V(III) center which serves to bridge the V–P–F–O layers.

The V(III) sites adopt a tetragonally distorted, axially elongated octahedral geometry. Each V(III) site bonds to two phosphate oxygens, one from each of two adjacent layers, in a *trans* orientation. The equatorial plane is defined by four aquo ligands. The V(III) oxidation state assignment is consistent with valence sum calculations (71) and with the charge requirements of the material. Thus, the gross structure of **1** · $2H_2O$ is reminiscent of that previously observed for $(H_3NCH_2CH_2NH_3)_{2.5}$ $[V(VO)_8(OH)_4(HPO_4)PO_4)_4(H_2O)_4] \cdot 2H_2O$ (56), which exhibits a structure constructed from V–P–O layers linked by V(III) octahedra.

The piperazinium cations and water molecules of crystallization occupy the void spaces between the layers and the V(III) buttresses. There is considerable hydrogen bonding

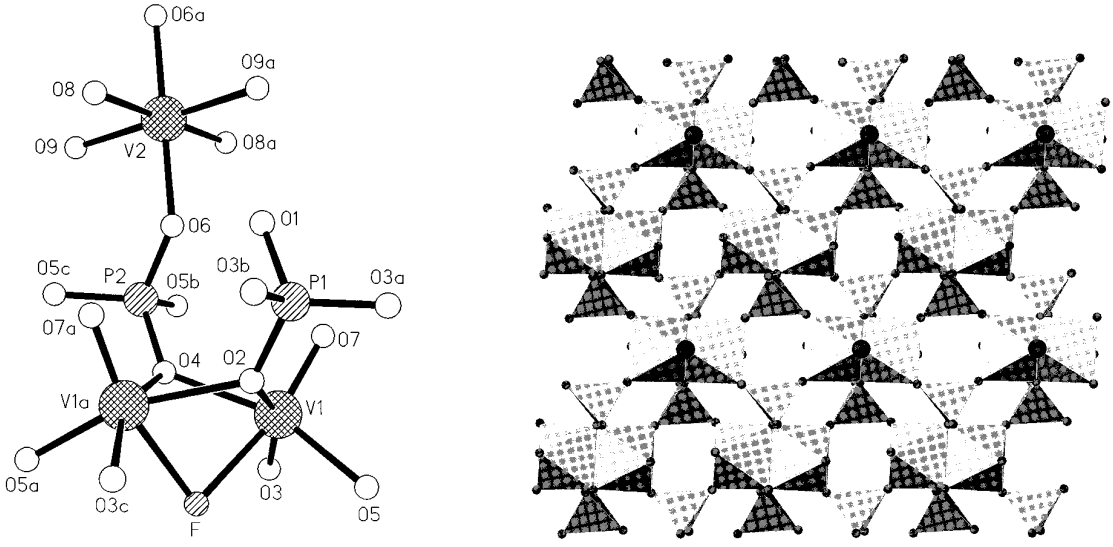

FIG. 2. (a) A view of the expanded asymmetric unit of the anionic framework of **1**, showing the confacial bioctahedral vanadium core of the layers and the atom-labeling scheme. (b) A polyhedral representation of the $(V^{IV}O)$–F^-–phosphate layers of **1**.

interaction between the cations, waters of crystallization, V(III) bound aquo ligands, and pendant {P–OH} groups of the layers. The presence of potentially labile aquo ligands suggests incipient vacant coordination sites within a micropore, whose properties appear to be dictated by a balance of hydrophilic/hydrophobic interactions which determine the manner in which such organic–inorganic solids can crystallize (72).

As shown in Fig. 4a, phosphate **2** · H_2O adopts a three-dimensional framework similar to that observed for **1** · $2H_2O$, constructed from a layer motif identical to that of **1** but with binuclear $\{(V^{IV}O)_2F_2O_6\}$ bridges replacing the $\{V^{III}O_6\}$ groups of **1**. The overall structure may be described in terms of edge- and face-sharing V(IV) binuclear units linked through phosphate tetrahedral into a three-dimensional anionic framework, providing interconnecting tunnels occupied by K^+ cations and water molecules of crystallization.

An unusual feature of the structure is the presence of two distinct V(IV) binuclear units and of three different V(IV) environments. One binuclear motif, *Type 2a*, is similar to that observed for **1** · $2H_2O$, consisting of a

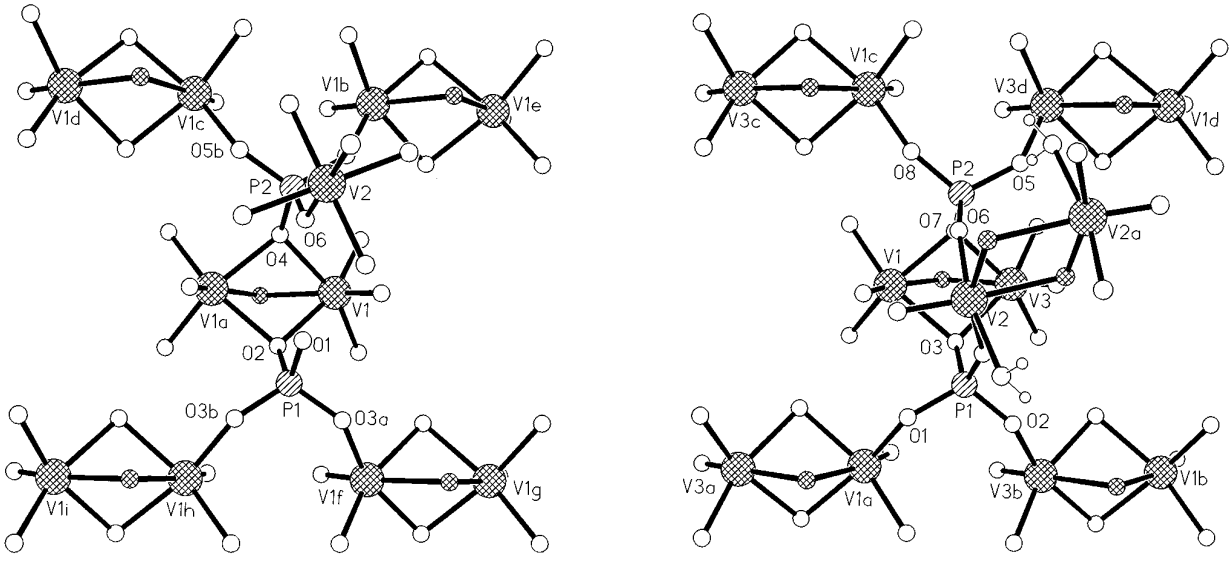

FIG. 3. (a) A view of the structure of **1**, normal to the $(V^{IV}O)$–F^-–phosphate layers, showing the distinct phosphorus sites, P1 and P2. (b) A similar view of the structure of **2**, illustrating that the layer motif is identical to that of **1** and showing the substitution of the $\{V^{III}O_6\}$ unit of **1** by $\{(V^{IV}O)_2F_2O_4\}$ bridges in **2**.

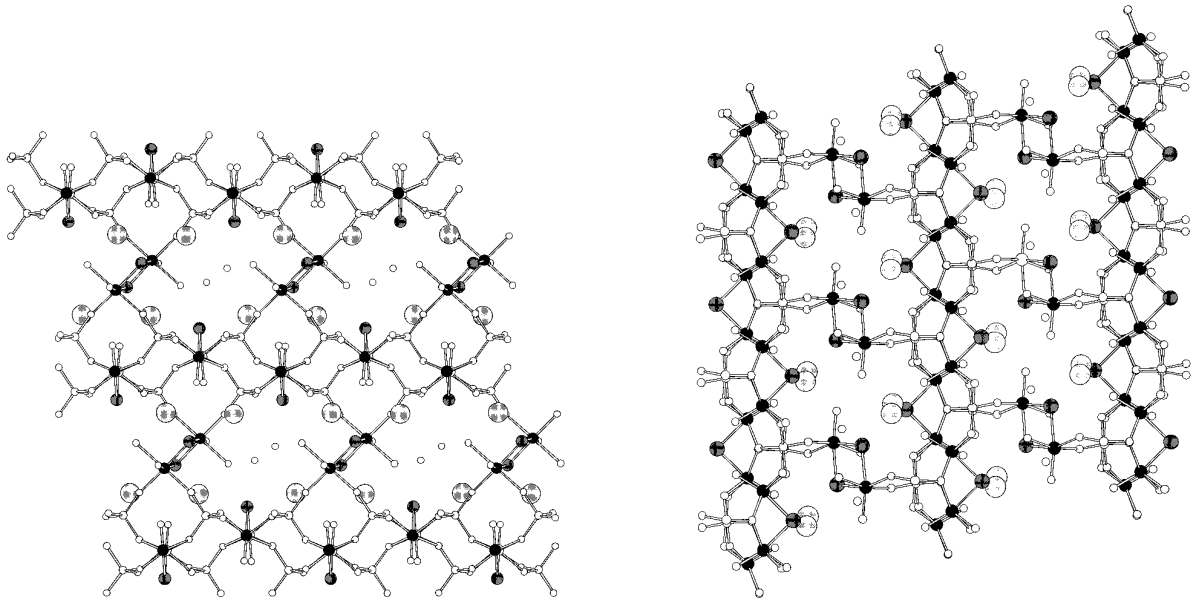

FIG. 4. (a) A view of the structure of **2**, illustrating the $(V^{IV}O)$–F^-–phosphate layers, bridged by $\{(V^{IV}O)_2F_2O_6\}$ units. (b) A view of the structure of **2** along the **c** axis, showing the channels occupied by the K^+ cations. Vanadium atoms are solid black spheres; fluoride sites are small grey spheres; potassium cations are large grey spheres.

confacial bioctahedral unit. Each V(IV) site of this unit coordinates to a terminal oxo-group, a bridging fluoride ligand, two bridging phosphate oxygen atoms from each of two phosphate groups, and two oxygen donors in a terminally bonding mode from two additional phosphate groups, as illustrated in Fig. 5. The second binuclear motif, *Type 2b*, consists of an edge-sharing unit, with each V(IV) geometry defined by *two* bridging fluorides, a terminal oxo-group, two terminal phosphate oxygen donors, and an aquo ligand.

It is noteworthy that the fluoride of the confacial bioctahedral unit is *trans* to both terminal oxo-groups, resulting in a symmetrical bridging interaction with V–F distances of 2.133(3) and 2.135(3) Å. In contrast, the fluoride bridges of the second binuclear site are *trans* to a single oxo-group, producing an unsymmetrical bridge with V-F distances of 1.983(3) Å and 2.180(3) Å. The geometries adopted by the binuclear units of **1** · $2H_2O$ and **2** · H_2O are compared to those of the prototypic material of this class $(H_3NCH_2CH_2NH_3)[(VO_2)_2(PO_4)F]$ (59) in Table 6. The structural versatility exhibited by this limited set of V–P–F–O materials is quite remarkable.

Each phosphate group provides an oxygen atom to bridge the vanadium sites of the confacial bioctahedral unit. Of the remaining three oxygen atoms, one is employed as a donor to a neighboring corner-sharing binuclear unit and two link to each of two adjacent Type 2a units. In this fashion, as illustrated in Fig. 3b, the

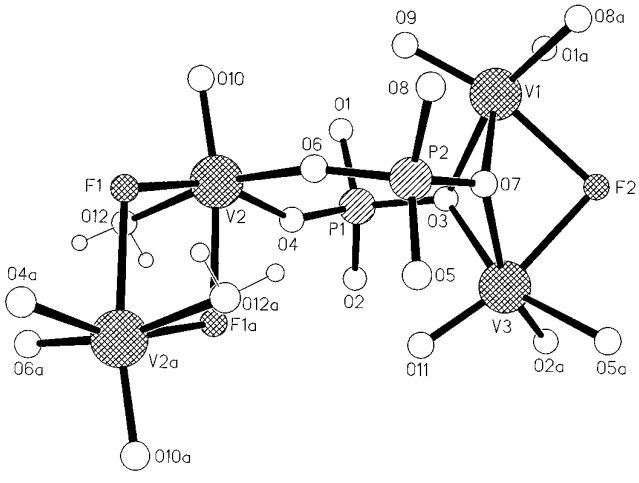

FIG. 5. A view of an expanded asymmetric unit of the anionic framework of **2**, showing the two distinct binuclear sites and the atom-labeling scheme.

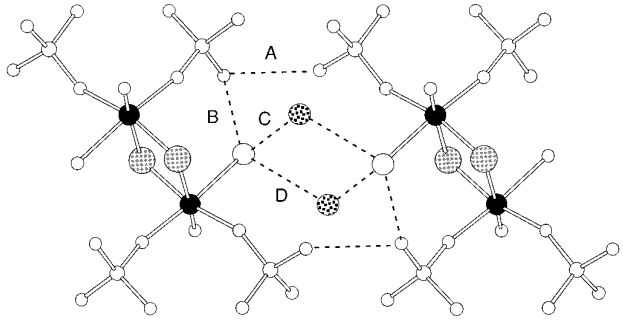

FIG. 6. The hydrogen-bonding network observed for **2**. Relevant distances (Å): A, 2.797; B, 2.708; C, 2.81; D, 2.911.

TABLE 6
Comparison of Selected Structural Parameters for the Vanadium Sites of Oxo-fluorovanadium Phosphate Phases[a]

Compound	Vanadium motif	Vanadium sites	V–O(oxo)	V–O(phosphate), ave.[b]	V–O(aquo)[b]	Valence	
						V–F	Sum
$[H_3NCH_2CH_2NH_3][(VO_2)_2(PO_4)F]$	Chains of corner-sharing {VO_5F} octahedra and {VO_4F} tetrahedra	V(oct)	1.607(5) 1.713(4)	2.011(4)(×3)		2.393(4)	4.72
		V(sq. pyp)	1.614(4) 1.676(4)	1.959(4)(x*L*)		1.924(4)	5.03
$[H_2N(C_2H_4)_2NH_2][V(VO)_4(HPO_4)_2(PO_4)_2F_2(H_2O)_4] \cdot 2H_2O$	Isolated V(III) octahedra and confacial bioctahedral V(IV) binuclear units	V(III)		1.987(8) (x*L*)	1.96(2)(×4)		3.12
		V(IV)	1.596(7)	2.030(7)(x4)		2.163(5)	4.07
$K_2[(VO)_3(PO_4)_2F_2(H_2O)] \cdot H_2O$	One confacial bioctahedral V(IV) binuclear unit (Type 2a) and one edge-sharing bioctahedral unit (Type 2b)	V(IV), Type 2a	1.598(4) 1.607(4)	2027(4)(×4) 2.031(4)(×4)		2.135(3) 2.133(3)	4.12 4.04
		V(IV), Type 2b	1.627(4)	1.943(4)(×2)	2.106(5)	1.983(3), 2.180(3)	4.12

[a] Bond lengths in Å.
[b] (x*n*): *n* refers to the number of bonds of the given type associated with the vandium site.
[c] Ref. (71).

phosphorus tetrahedra serve to bridge each Type 2a binuclear unit to one Type 2b and four Type 2a neighbors.

When viewed along the crystallographic a axis as in Fig. 4a, this complex connectivity pattern produces channels defined by a 10-polyhedral ring. The water molecules of crystallization occupy those channels, and the aquo ligands of the Type 2b sites project into the cavity, resulting in significant hydrogen bonding between the various water molecules. When the structure is projected down the **b** axis, as in Fig. 4b, a second set of channels is revealed. These intersect the first set and the location of K^+ cations within these tunnels is clearly observed. A 12-polyhedral ring defines the perimeter of this latter set of tunnels. As shown in Fig. 6, there is significant hydrogen bonding between the phosphate oxygens, aquo ligands, and water molecules of crystallization. It is also noteworthy that the interiors of the channels in **2** contain chains of fluoride-bridged K^+ cations with K–F distances of 2.78 Å; this distance may be compared to that of 2.67 Å in KF.

CONCLUSIONS

The metal-mediated hydrolysis of fluorophosphoric acid provides a convenient and effective method for introducing fluoride into the anionic framework of V–P–F–O phases. These oxyfluoridevanadophosphate materials exhibit a remarkable structural diversity, which reflects the flexibility of coordination polyhedron available to the vanadium sites, the variable oxidation states accessible to vanadium, and the multifarious connectivity patterns which may be adopted by corner-, edge-, and face-sharing polyhedra. By combining the chemical stability of an oxide framework and the enhanced mechanical thermal stability endowed by fluoride incorporation, with the presence of incipiently coordinatively unsaturated transition metal sites, a new class of potentially microporous materials has emerged which may provide access to synthetic routes to designed materials.

Tables of experimental conditions for the X-ray studies, atomic positional parameters, bond lengths and angles and observed and calculated structure factors for $\mathbf{1} \cdot 2H_2O$ and $\mathbf{2} \cdot H_2O$ are available from the authors upon request.

ACKNOWLEDGMENT

The work at Syracuse University was funded by NSF Grant CHE9318824.

REFERENCES

1. H. Seeboth, B. Kubias, H. Wolf, and B. Luche, *Chem. Tech* **28,** 730 (1976).
2. E. Bordes and P. Courtine, *J. Chem. Soc. Chem. Commun.*, 294 (1985).
3. G. Centi, F. Trifiro, J. R. Ebner, and V. M. Franchetti, *Chem. Rev.* **88,** 55 (1988).
4. J. Haggin, *Chem. Eng. News*, 20, April 3 (1995).
5. P. L. Gai and K. Kourtakis, *Science* **267,** 661 (1995).
6. M. Tachey, F. Theobold, and E. Bordes, *J. Solid State Chem.* **40,** 280 (1981).
7. E. Bordes, P. Courtine, and G. Pannetier, *Ann. Chim.* **8,** 105, (1973).
8. B. D. Jordan and C. Calvo, *Can. J. Chem.* **51,** 2621 (1973).
9. Yu E. Gorbimova and S. A. Linde, *Sov. Phys. Dokl.* (*Engl. Transl.*) **24,** 138 (1979).
10. C. C. Torardi and J. C. Calabrese, *Inorg. Chem.* **23,** 1308 (1984).

11. A. LeBail, G. Férey, P. Amoros, and D. Beltran-Porter, *Eur. J. Solid State Chem.* **26,** 419 (1989).
12. A. LeBail, G. Férey, P. Amoros, D. Beltran-Porter, and G. Villeneune, *J. Solid State Chem.* **79,** 169 (1989).
13. M. E. Leoniwicz, J. W. Johnson, J. F. Brody, H. F. Shannon, and J. M. Newsom, *J. Solid State Chem.* **56,** 370 (1985).
14. J. W. Johnson, D. C. Johnston, H. E. King, Jr., T. R. Halbert, J. F. Brody, and D. P. Goshorn, *Inorg. Chem.* **27,** 2646 (1988).
15. P. Amoros, D. Beltran-Porter, A. LeBail, G. Férey, and G. Villeneuve, *Eur. J. Solid State Chem.* **25,** 599 (1988).
16. P. Amoros and A. LeBail, *J. Solid State Chem.* **97,** 283 (1992).
17. G. Huan, J. W. Johnson, A. J. Jacobson, E. W. Corcoran, and D. P. Goshorn, *J. Solid State Chem.* **93,** 514 (1991).
18. K. H. Lii, N. S. Wen, C. C. Su, and B. R. Chueh, *Inorg. Chem.* **31,** 439 (1992).
19. W. T. A. Harrison, J. T. Vaughey, A. J. Jacobson, D. J. Goshorn, and J. W. Johnson, *J. Solid State Chem.* **116,** 77 (1995).
20. H.-Y. Kang, S.-L. Wang, P.-P. Tsai, and K. H. Lii, *J. Chem. Soc. Dalton Trans.* 1525 (1993).
21. H. Y. Kang, S. L. Wang, and K. H. Lii, *Acta Cryst.* **C48,** 975 (1992).
22. K. H. Lii, H. J. Tsai, and S. L. Wang, *J. Solid State Chem.* **87,** 396 (1990).
23. Yu E. Gorbunova, S. A. Linde, A. V. Lavrov, and I. V. Tananaev, *Dohl. Akad. Nank SSSR* **250,** 350 (1980).
24. K. H. Lii and S. L. Wang, *J. Solid State Chem.* **82,** 239 (1989).
25. K. H. Lii and H. J. Tsai, *Inorg. Chem.* **30,** 446 (1991).
26. S. L. Wang, H. Y. Kang, C. Y. Cheng, and K. H. Lii, *Inorg. Chem.* **30,** 3496 (1991).
27. R. C. Haushalter, Z. Wang, M. E. Thompson, J. Zubieta, and C. J. O'Connor, *Inorg. Chem.* **32,** 3966 (1993).
28. D. Lozano-Calero, S. Bruque, M. A. G. Aranda, M. Martinez-Lara, and L. Moreno, *J. Solid State Chem.* **103,** 481 (1993).
29. R. C. Haushalter, Q. Chen, V. Soghomonian, J. Zubieta, and C. J. O'Connor, *J. Solid State Chem.* **108,** 128 (1994).
30. R. C. Haushalter and J. Zubieta, unpublished results.
31. M. L. F. Phillips, W. T. A. Harrison, E. G. Thurman, G. Stucky, G. V. Kulkarni, and J. K. Burdett, *Inorg. Chem.* **29,** 2158 (1990).
32. L. Benhamada, A. Grandin, M. M. Borel, and B. Raveau, *Acta Cryst.* **C47,** 1138 (1991).
33. A. Grandin, J. Chardon, M. M. Borel, A. Leclaire, and B. Raveau, *J. Solid State Chemistry* **99,** 297 (1992).
34. A. Leclaire, H. Chahboun, D. Groult, and B. Raveau, *J. Solid State Chem.* **77,** 170 (1988).
35. K. H. Lii, Y. P. Wang, and S. L. Wang, *J. Solid State Chem.* **80,** 127 (1989).
36. R. C. Haushalter, Z. Wang, M. E. Thompson, and J. Zubieta, *Inorg. Chim. Acta* **232,** 83 (1995).
37. R. C. Haushalter, Z. Wang, M. E. Thompson, and J. Zubieta, *Inorg. Chem.* **32,** 3700 (1993).
38. A. Benmoussa, M. M. Borel, A. Grandin, A. Leclair, and B. Raveau, *J. Solid State Chem.* **97,** 314 (1982).
39. L. Benhamada, A. Grandin, M. M. Borel, A. Leclaire, and B. Raveau, *J. Solid State Chem.* **94,** 274 (1991).
40. A. Leclaire, J. Chardon, A. Grandin, M. M. Borel, and B. Raveau, *J. Solid State Chem.* **108,** 291 (1994).
41. A. LeBail, M. LeBlanc, and P. Amoros, *J. Solid State Chem.* **87,** 178 (1990).
42. J. T. Vaughey, T. A. Harrison, and A. J. Jacobson, *J. Solid State Chem.* **110,** 305 (1994).
43. L. Benhamada, A. Grandin, M. M. Borel, A. Leclaire, and B. Raveau, *J. Solid State Chem.* **97,** 131 (1992).
44. K. H. Lii and C. S. Lee, *Inorg. Chem.* **29,** 3298 (1990).
45. C. E. Rice, W. R. Robinson, and B. C. Tofield, *Inorg. Chem.* **15,** 345 (1976).
46. K. H. Lii and L. F. Mao, *J. Solid State Chem.* **96,** 436 (1992).
47. R. C. Haushalter, V. Soghomonian, Q. Chen, and J. Zubieta, *J. Solid State Chem.* **105,** 512 (1993).
48. S. Boudin, A. Grandin, A. Leclair, M. M. Borel, and B. Raveau, *J. Solid State Chem.* **111,** 365 (1994).
49. J. Huang, Q. Gu, and A. Sleight, *J. Solid State Chem.* **110,** 226 (1994).
50. K. H. Lii and W. C. Liu, *J. Solid State Chem.* **103,** 38 (1993).
51. A. Grandin, J. Chardon, M. M. Borel, A. Leclaire, and B. Raveau, *J. Solid State Chem.* **104,** 226 (1993).
52. P. Crespoa, A. Grandin, M. M. Borel, A. Leclaire and B. Raveau, *J. Solid State Chem.* **105,** 307 (1993).
53. M. I. Khan, L. M. Meyer, R. C. Haushalter, A. L. Schweitzer, J. Zubieta, and J. L. Dye, *Chem. Mater.* **8,** 43 (1996).
54. V. Soghomonian, R. C. Haushalter, Q. Chen, and J. Zubieta, *Inorg. Chem.* **33,** 1700 (1994).
55. V. Soghomonian, R. C. Haushalter, Q. Chen, and J. Zubieta, *Science* **256,** 1596 (1993).
56. V. Soghomonian, R. C. Haushalter, Q. Chen, and J. Zubieta, *Angew. Chem. Int. Ed. Eng.* **32,** 610 (1993).
57. V. Soghomonian, R. C. Haushalter, Q. Chen, and J. Zubieta, *Chem. Mater.* **5,** 1690 (1993).
58. V. Soghomonian, R. C. Haushalter, Q. Chen, and J. Zubieta, *Chem. Mater.* **5,** 1595 (1993).
59. D. Riou and G. Férey, *J. Solid State Chem.* **120,** 137 (1995).
60. T. Loiseau and G. Férey, *J. Solid State Chem.* **111,** 416 (1994).
61. X. Bu, P. Feng, and G. D. Stucky, *J. Chem. Soc., Chem. Commun.*, 1337 (1995).
62. T. Loiseau and G. Férey, *Eur. J. Solid State Chem.* **30,** 369 (1993).
63. T. Loiseau and G. Férey, *J. Chem. Soc. Chem. Commun.*, 1197 (1992).
64. X. Yin and L. F. Nazar, *J. Chem. Soc., Chem. Commun.*, 2349 (1994).
65. D. Riou and G. Férey, *J. Solid State Chem.* **111,** 422 (1994).
66. N. Walker and D. Stuart, *Acta Crystallogr. Sect. A* **39,** 158 (1983).
67. "teXsan: Texray Structural Analysis Package," revised. Molecular Structure Corporation, The Woodlands, TX, 1992.
68. D. T. Cromer and J. T. Weber, "International Tables for X-Ray Crystallography," Vol. IV. Kynoch Press, Birmingham, England, 1974.
69. D. C. Creagh and J. W. J. McAuley, "International Tables for X-Ray Crystallography," Vol. C. Table 4,.2.6.8. Kluwer Academic, Boston, 1992.
70. SHELXTL PC, Siemens Analytical X-Ray Instruments, Inc., Madison, WI, 1990.
71. I. D. Brown, *in* "Structure and Bonding" (M. O'Keefe and A. Novrotsky, Eds.), Vol II, Academic Press, New York, 1981.
72. R. C. Haushalter and L. A. Mundi, *Chem. Mater.* **4,** 31 (1992).